



# Lawrence Berkeley Laboratory

UNIVERSITY OF CALIFORNIA

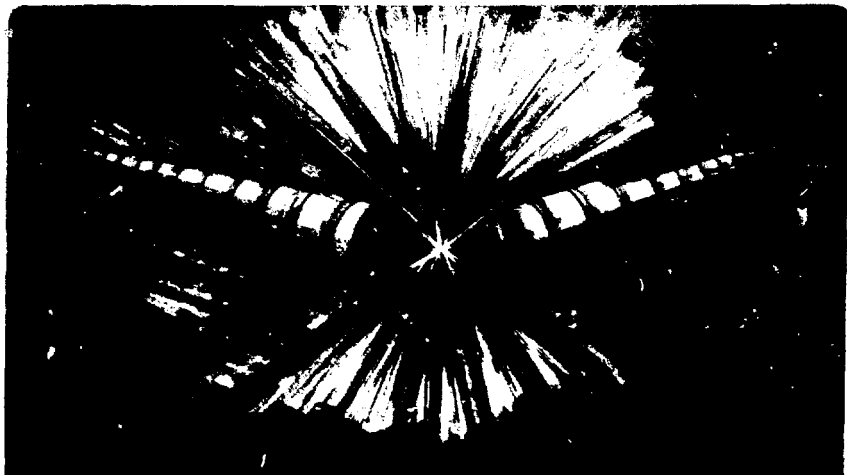
## Accelerator & Fusion Research Division

Presented at the 3rd International Symposium on the  
Production and Neutralization of Negative Ions and  
Beams, Brookhaven National Laboratory, Upton, NY,  
November 11-18, 1983

THE STATUS OF 1 AMPERE  $H^-$  ION SOURCE DEVELOPMENT AT  
THE LAWRENCE BERKELEY LABORATORY

A.F. Lietzke, K.W. Ehlers, and K.N. Leung

November 1983



# THE STATUS OF $>1$ AMPERE $H^-$ ION SOURCE DEVELOPMENT AT THE LAWRENCE BERKELEY LABORATORY

A.F. Lietzke, K.W. Ehlers and K.N. Leung  
Lawrence Berkeley Laboratory  
University of California  
Berkeley, CA 94720

## INTRODUCTION

This paper summarizes the effort to improve the operation of the  $\sim 1$  A surface-production  $H^-$  ion source developed by K.W. Ehlers and K.N. Leung. The plasma chamber consists of a large magnetic bucket of oval cross section (Fig. 1). A concave cylindrical "converter" surface is suspended in the plasma chamber to direct any surface-produced negative ions through the exit aperture. The ion source has been mated to a tetrode accelerator for the "proof-of-principle" tests. Most of the problems discovered in the tests were associated with difficulties in controlling the production process. This paper describes the plasma chamber in greater detail and illustrates the quality of the present ion production. The acceleration difficulties have been deferred until a better test-stand is completed.

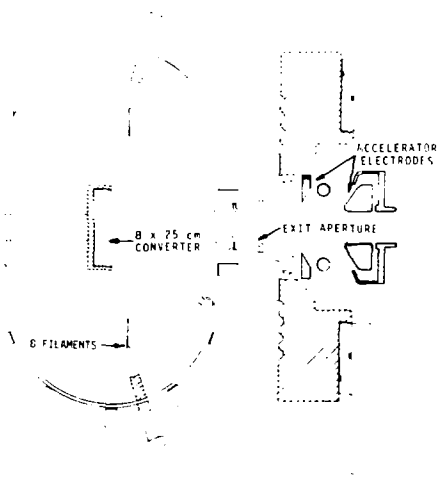


Figure 1  
Schematic of  
LBL  $\sim 1$  A  $H^-$   
surface-production  
ion source,  
showing the con-  
verter in rela-  
tion to the  
filaments, the  
exit aperture,  
and the accel-  
erator elec-  
trodes.

LBL 817-107456

## PLASMA CHAMBER DESCRIPTION

The plasma chamber cathode consists of eight filaments (1.5 mm diameter tungsten) having a total emission area of  $\sim 55 \text{ cm}^2$ . They are distributed uniformly in two magnetic field nulls (Fig. 2) which run parallel to the cylindrical axis of the chamber's anode wall. The anode is shielded by line cusps (total length = 950 cm) in the form of six hoops and two isolated lines of samarium-cobalt magnets. A weak filter ( $\sim 50 \text{ G-cm}$ ) separates the filament null from the converter nulls, which are separated by  $\sim 300 \text{ G-cm}$  from the aperture null and  $\sim 1200 \text{ G-cm}$  from the wall nulls.

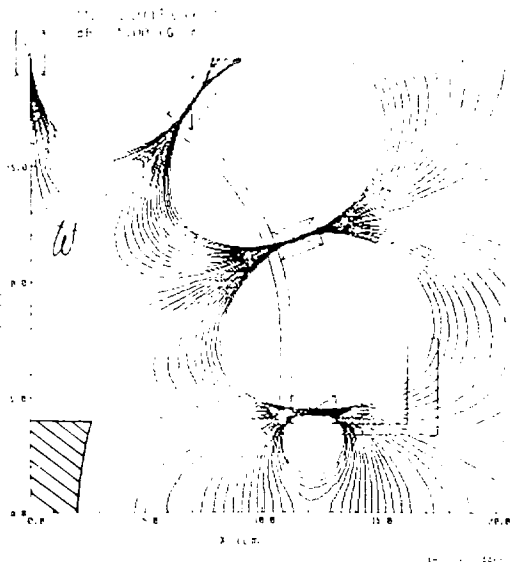
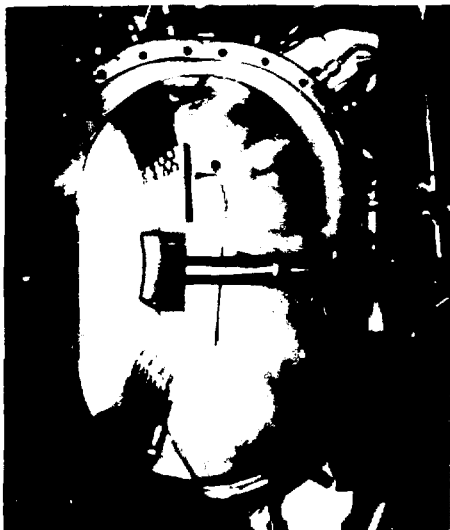


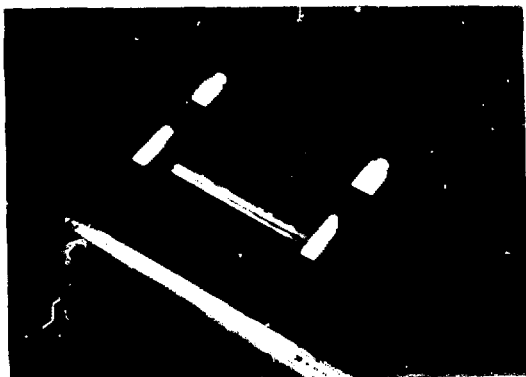
Figure 2  
Calculated  
magnetic field  
structure in one  
quadrant of the  
plasma chamber  
showing the  
filament filter  
and exit filter  
in relation to  
the filaments  
and the con-  
verter.

The negative ions created on the converter ( $-130 \text{ V}$  relative to the anode) are accelerated in the plasma sheath and penetrate the exit filter with a small displacement ( $\sim 2 \text{ cm}$ ) parallel to the cylindrical axis. The converter is roughly in the center of the plasma chamber (Fig. 3), being suspended by its water cooling pipes. The exit surface (molybdenum) is brazed onto a copper substrate which runs cold but is shielded by two hot molybdenum shields (Figs. 4 and 5). The inner shield is at the converter potential (with the intention of being hot enough to stay clean) while the outer shield floats (thereby reducing the converter power supply requirement) and protects the intermediate boron nitride insulator from plasma bombardment and tungsten deposition.



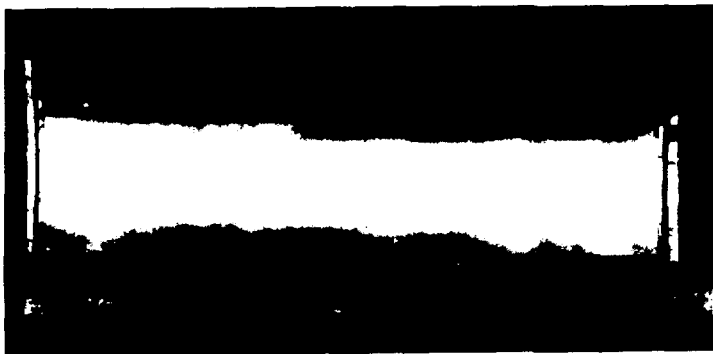
CB8830-8753

Figure 3 End photo showing the converter and its shields in relation to the filaments and the large epoxy accelerator insulator.



CB8 330-8741

Figure 4 Photo of the converter and its insulated box (separated for detailed observation).



CBB 830-8743

Figure 5 Exit view of the 8 x 25 cm converter showing the outer shields in operating position.

Both shields are creased and constrained in a manner to minimize warpage while hot.

Cesium has been injected at three locations. At this writing, it is being injected behind the converter, from one end-plate where the injector (Fig. 6) mounts onto a standard flange. The injector has a high temperature needle-valve which separates the cesium reservoir from the main vacuum. Both the valve and the reservoir operate inside a temperature-controlled oven (250 - 270 °C). The cesium vapor is conducted to the plasma chamber by an ohmically heated tube.

An inter-cusp cage is being used to test theories of cesium transport. It enhances the H<sup>-</sup> output only when it is negative (~50 V, 4 A) and the walls are somewhat loaded with cesium. The H<sup>-</sup> uniformity is diagnosed by a movable, screened, faraday cup operated with the screen 12 V below anode and the cup 24 V above anode (sufficient for the cup current to be composed of only fast H<sup>-</sup> and secondary electrons from the screen).

#### OPERATION

At the standard "no cesium" operating point, there is 9 kW of arc power (90 V, 100 A), 1.2 kW of converter power (150 V, 8A) and 5 kW of filament power (8 filaments x 7.5 V, 100 A). This produces an output current in the neighborhood of 20-50 mA. Optimum injection of cesium (without other changes) nearly doubles the converter current (14 A), raises the arc current 20% and delivers over 1 A through the exit throat. Fig. 7 is raw data illustrating typical operation after the plasma system is well-conditioned. This data was collected after five hours of continuous operation at the 1 A output level, so when the arc is turned ON, the floating converter produces some H<sup>-</sup> energetically

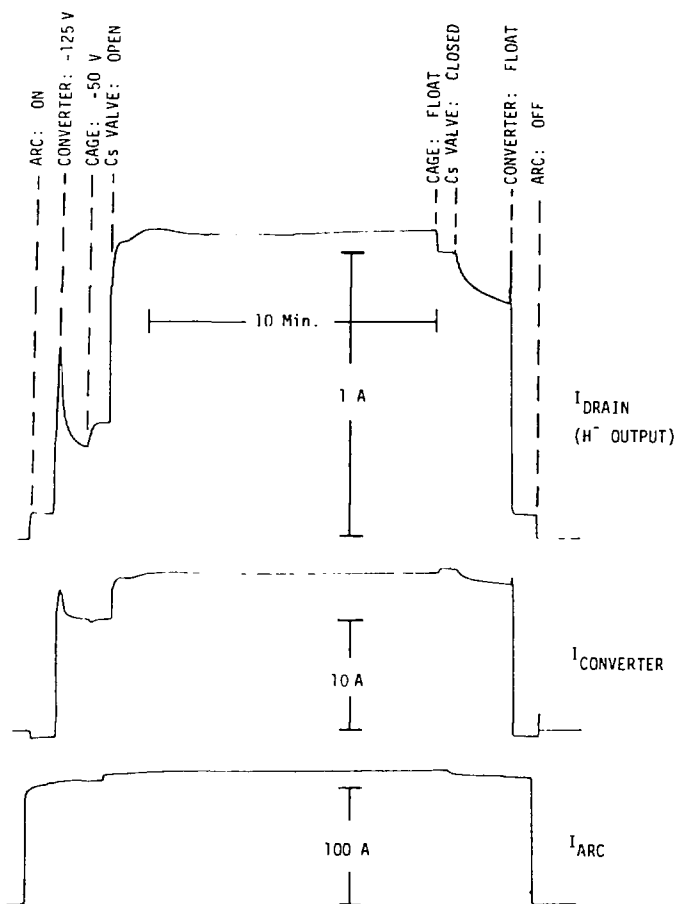


Figure 6 The cesium injector consists of a high temperature regulating valve which separates the reservoir from the ohmically-heated tube leading to the main plasma chamber.

CBB 830-8747

capable of penetrating the exit filter. Biasing the converter to its previous optimum produces a rapidly rising, but short-lived, surge of  $H^-$  (as the accumulated cesium is depleted). Biasing the cage to its previous optimum yields another 100 mA increase. The big increase in  $H^-$  occurs  $\sim 1$  sec after the cesium valve is opened. Steady state is attained in  $\sim 1$  minute and maintained for 10 minutes by slowly closing the cesium supply valve. Shutdown in this history was initiated by first floating the cage (to check its effect under steady Cs input conditions). Closing the cesium valve immediately starts the decay of the  $H^-$  output (the slope is utilized to estimate the cesium "pumping" time). "Refloating" the converter produces another (but smaller) surge in  $H^-$  (as the converter passes through its optimum coverage again). The following negative converter current results from electron collection caused by a "load" resistor to anode. It disappears when the arc is extinguished.

Fig. 8 shows some profiles taken under optimum cesium conditions. These are not "typical" profiles (which suffer from non-uniform cesiation) but they illustrate the vignetting and attenuation the  $H^-$  beam suffers before arrival at the accelerator aperture ( $z = 18$  cm). The non-uniform cesiation is inversely related to the positive ion variation (Sputtering and cesium ionization are believed to be the mechanisms.) The focal plane non-uniformity in the focussed direction depends only upon the transverse



XBL 8311-4467

Figure 7 Standard operating sequence: 18 minutes from arc on to arc off, including converter on, cage on, cesium valve open. ~10 minutes where the cesium valve was slowly closed to maintain a steady output, cage off, cesium valve closed, converter off, arc off.

$\text{H}^-$  temperature (a good fit is obtained by assuming a 6 eV Gaussian velocity distribution) and the vignetting of the exit aperture.

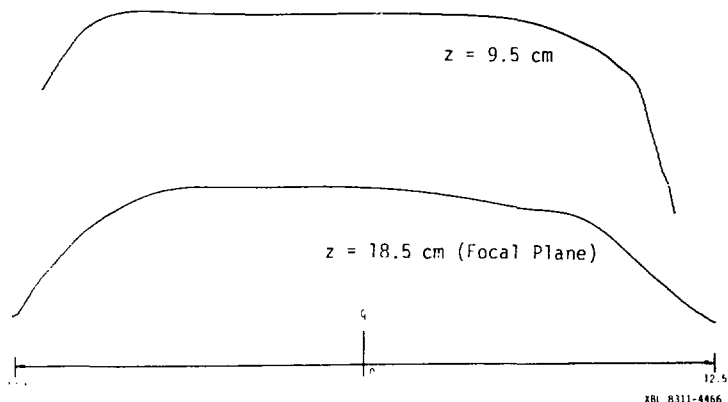


Figure 8 The  $H^-$  intensity, parallel to the converter axis, suffers from vignetting and attenuation (in spite of geometric focusing). Profiles were taken at  $I_{\text{drain}} \approx 1$  ampere within four minutes of each other under very steady conditions. These are not typical profiles (which also suffer from non-uniform cesiation).

#### ENGINEERING EFFORT

Hardware modifications consumed much of the past year, but have recently permitted controlled and reproducible behavior (of the type shown in Fig. 7, 8). Modifications were indicated by the types of problems identified in the "proof-of-principle" tests:

1. Lack of  $H^-$  steadiness (caused by strong coupling between a poorly controlled cesium feed system and the filament emission).
2. Lack of  $H^-$  steadiness (caused by frequent cathode spotting from the converter and filaments, which produced large cesium transients on the converter).
3. Heavy cesium consumption (necessitating frequent clean-up and frequent spotting).

#### PHYSICS EFFORT

Some phenomena are not yet "explained"; some are not even reproducible enough to study, but some, like the profiles, seem well understood. Others, like the high cesium consumption rate, the anomalously high cesium reservoir temperatures, the causes of the  $H^-$  attenuation, the mechanism(s) for electron leakage, variations in the optimum converter voltage, and the non-linear input/output relations, remain subjects of speculation and investigation.



## CONCLUSIONS

The system, as it stands, works very well up to 1.3 A. Indeed, the hardware is recently capable of controlled experimentation. Investigations are believed to be necessary to examine engineering trade-offs, and push-out (or remove) fundamental limitations. Some hardware improvements already await testing and upcoming beam tests may reveal new problems.

## ACKNOWLEDGEMENTS

Bill Yant and Carolyn Wong deserve special attention for working so well under adverse conditions: Bill for his help with the modifications and data collection, and Carolyn, for her help with this manuscript.

This work was supported by the Director, Office of Energy Research, Office of Fusion Energy, Development and Technology Division of the U.S. Department of Energy under Contract No. DE-AC03-76SF00098.

## DISCLAIMER

This report was prepared as an account of work sponsored by an agency of the United States Government. Neither the United States Government nor any agency thereof, nor any of their employees, makes any warranty, express or implied, or assumes any legal liability or responsibility for the accuracy, completeness, or usefulness of any information, apparatus, product, or process disclosed, or represents that its use would not infringe privately owned rights. Reference herein to any specific commercial product, process, or service by trade name, trademark, manufacturer, or otherwise does not necessarily constitute or imply its endorsement, recommendation, or favoring by the United States Government or any agency thereof. The views and opinions of authors expressed herein do not necessarily state or reflect those of the United States Government or any agency thereof.

This report was done with support from the Department of Energy. Any conclusions or opinions expressed in this report represent solely those of the author(s) and not necessarily those of The Regents of the University of California, the Lawrence Berkeley Laboratory or the Department of Energy.

Reference to a company or product name does not imply approval or recommendation of the product by the University of California or the U.S. Department of Energy to the exclusion of others that may be suitable.